geosciences

MDPI

Article

Induced Seismic-Site Effects on the Vulnerability Assessment of a Historical Centre in the Molise Region of Italy: Analysis Method and Real Behaviour Calibration Based on 2002 Earthquake

Nicola Chieffo [1] and Antonio Formisano [2,*]

[1] Faculty of Architecture and Urbanism, Politehnica University of Timişoara, 300223 Timişoara, Romania; nicola.chieffo@student.upt.ro
[2] Department of Structures for Engineering and Architecture, School of Polytechnic and Basic Sciences, University of Naples "Federico II", 80125 Naples, Italy
* Correspondence: antoform@unina.it

Received: 2 December 2019; Accepted: 30 December 2019; Published: 3 January 2020

Abstract: The present research aims to estimate the influence of site amplification on the seismic vulnerability of the historical centre of the municipality of Baranello in the Molise Region of Italy. Firstly, a structural and typological characterization of the investigated area has been done according to the EMS-98 scale. Subsequently, the vulnerability assessment of the historical buildings located there has been carried out through an appropriate survey form in order to identify the buildings which are most susceptible to seismic damage. To this purpose, the seismic event occurring in October of 2002 has been selected as a reference earthquake. Moreover, according to the AeDES form implemented by the Italian Civil Protection Department to evaluate the usability of constructions after seismic events, the calibration of the typological vulnerability curves of the built-up area has been done, and a quantitative assessment of the local seismic response has been achieved, based on the seismic motions recorded after the 2002 Molise earthquake. Finally, the local amplification factor, which negatively influences the severity of the seismic damage on the structures, has been taken into account in order to more correctly foresee the expected damage of the inspected urban sector, so as to use more appropriately the achieved results for reliable seismic risk mitigation plans.

Keywords: site-effects; vulnerability assessment; masonry building compounds; damage scenarios; calibrated vulnerability curves

1. Introduction

The recent tragic earthquakes which have occurred in Italy during the last decades are a living testimony of the bad seismic behaviour of the historical centres of many municipalities. This is due to a series of hazardous factors, such as the age of buildings, the poor quality of materials and the insufficient maintenance of constructions, which lead towards the high seismic vulnerability of several built-up areas. In fact, the seismic vulnerability of a given built area indicates the expected amount of damage triggered by an earthquake of a specific magnitude [1]. Therefore, the seismic vulnerability assessment of an urban environment is devoted to estimating the capacity of the built-up area to withstand without failures a series of seismic events, which are responsible for huge economic losses and casualties.

Generally, in an overall perspective, the Vulnerability (V), through a multi-factorial combination with other two parameters, namely Exposure (E) and Hazard (H), leads towards the definition of the seismic risk, which can have direct or indirect influence on a specific area.

Reducing the seismic risk requires researchers to assess the seismic behaviour of buildings towards earthquakes (Vulnerability), the amount of human and material resources that could be lost in the case of seismic events (Exposure) and the intensity and recurrence of earthquakes (Hazard).

In fact, focusing on the urban scale, rapid urbanization has dramatically increased the vulnerabilities and risks of urban dwellers in densely populated areas. The high population, combined with the presence of numerous buildings that do not comply with seismic regulations, significantly increase the problem of seismic safety in urbanized areas [2,3].

At urban-scale, the management of a large number of variables, such as different types of buildings, people, roads, etc., is an important issue to accomplish, since the expected damage probability must be foreseen.

The identification of the most vulnerable buildings in an urban context is not a simple task due to their heterogeneity and complexity. In general, the predisposition of a building to be damaged by a seismic impact depends upon many aspects that are mainly concerned with the type of construction, the quality of the materials used, the construction methods and the preservation state. Many studies [4–6] have shown that the lack of these features make structures ineffective against earthquakes. In fact, masonry buildings especially, which are located within historic centres, are very often characterized by a static inadequacy, mainly due to antiquated and unsuitable construction techniques, which do not guarantee an adequate security level. To this purpose, an inventory of buildings is an essential procedure for the acquisition of data aiming at evaluating the large-scale seismic vulnerability [7,8].

The available strategies usually take into consideration survey forms [9,10] to collect information on historical centre buildings mainly based on several seismic parameters, i.e., the seismic-resistant system type to lateral loading, the structural regularity, the maintenance conditions and the presence of existing damages. The application of these survey forms allows us to fully understand the various structural types located within heterogeneous urban centres [11].

Thus, in this perspective, the impact of an earthquake can be assessed in terms of expected losses. Therefore, the formulation of an earthquake loss model in a given region is not only of interest for the economic impact of future earthquakes, but it is also important for risk mitigation. A specific loss model makes possible to predict damage to the built environment for a specific data scenario, in the framework of a deterministic approach model, and can be particularly important for responding to emergencies planning with targeted actions in order to safeguard people and the historical heritage of a given area [12–14].

Nowadays, the evaluation of the geological effects has been taken into consideration in the framework of risk assessment in order to have a better and correct forecast of the expected damage [15]. In this circumstance, the soil layers amplify or reduce the seismic waves on the crustal surface. Site effects are thus dangerous when the amplification of seismic waves in surface geological layers occurs. In fact, surface motion can be strongly amplified if geological conditions are unfavourable [16].

Generally, specific geological, geomorphologic and geo-structural settings of restricted areas can induce a high level of shaking on the ground surface even in occasions of low-intensity/magnitude earthquakes. This effect is called site or local amplification. Furthermore, the characterization of site effects can be carried out considering the ground model as a one-dimensional (1D) or two-dimensional (2D) half-space. The substantial difference between the two ground models is that in a 1D analysis, only the depth of the half-space is taken into consideration, neglecting the lateral confinement effect. On the other hand, the more accurate 2D analysis takes into account the significant volume of the soil in the longitudinal and vertical directions. The study of site effects can be conducted using two distinct approaches, namely time domain or frequency domain. In the first case, the local amplification factor is estimated by means of the time sequence (time history) at the bedrock with respect to the amplification at the ground surface. In the second case, the amplification coefficient is achieved considering the Fourier amplitude spectra or the response spectrum [17].

A reliable and easy method for large scale analysis developed by Giovinazzi [15] and Chieffo and Formisano [18] allows us to estimate the macroseismic intensity increment derived from specific

soil category, so as to properly define, taking into account the local amplification factors, the global vulnerability of building stocks according to the EMS-98 scale.

Based on these considerations, the municipality of Baranello, in the province of Campobasso, has been selected as a case study to evaluate the possible damages under seismic events.

The proposed work aims to evaluate the local amplification effects considering the time domain of a 1D half-space ground model. The main goal of this work is to investigate the influence of soil amplification on the seismic behaviour of typical masonry aggregates with the final target to plot the damage scenarios expected under different earthquake moment magnitudes and site–source distances.

2. The Municipality of Baranello

2.1. The Historical Background

Baranello (Figure 1) is a small town located in the province of Campobasso in the Molise Region of Italy. The municipality has 2759 inhabitants and rises at 610 m above sea level with an extended area of 25 km^2. The town has medieval origins, and it is bordered by the towns of Busso, Colle d'Anchise, Spinete and Vinchiaturo.

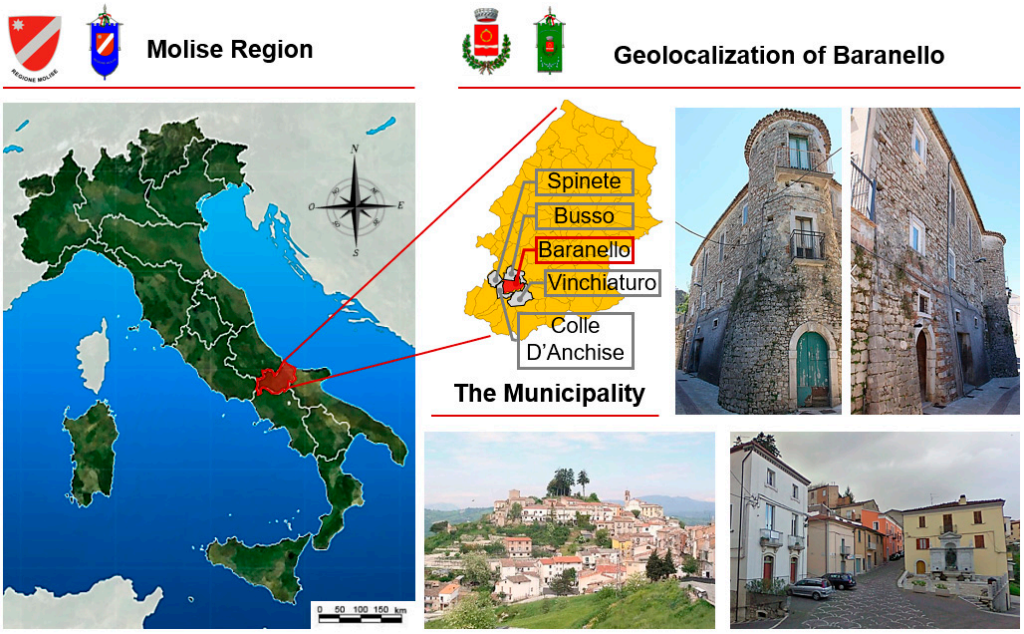

Figure 1. The geographical localization of the municipality of Baranello.

There is limited historical information about the evolution of the centre during time. The village was mentioned for the first time in the fourteenth century as a possession of Capece Galeota dating back to Norman ages. Only in 1591 the feud was sold by the Carafa family (one of whom had been Pope Paul IV) to the Marquis and then to Angelo Barone. Until the nineteenth century, Baranello was part of the Aragonese domain, and finally of the Ruffo family. One example of Norman architecture is the Ruffo castle, owned by the homonymous family until the nineteenth century. It was built at the highest point of the ancient village, performing its function of defence and control of the entire territory. It is inserted inside a building complex that puts it in communication with the tower, which represents the highest part of the construction.

Nowadays, the territory presents the characteristics of a mountain centre: narrow and steep streets that become wider and easier towards the area of new settlement. The urban centre is characterized by houses, that preserve their original appearance and are located around the church and along the main streets, while the modern buildings are placed in other districts belonging to the municipal territory [19].

2.2. The 2002 Molise Seismic Event Occurred on 31 October

The 2002 Molise earthquake was a significant event which historically occurred on 31 October 2002, with the epicentre localized in the province of Campobasso between the municipalities of San Giuliano di Puglia, Colletorto, Santa Croce di Magliano, Bonefro, Castellino del Biferno and Provvidenti. This event, having magnitude M_w = 5.7, was perceived in a large area of Central-Southern Italy, causing significant damage in a restricted area between Frentani, Sannio and Foggia (Figure 2) [20–22].

The source of the earthquake was located about 20 km from a deep seismogenic structure located below the Apula Platform. The replicas (aftershocks, more than 1900 seismic events) showed a predominantly vertical seismogenic structure, between 10 and 25 km deep, oriented in an east–west direction and consisting of two main segments having a length of about 15 km each. Moreover, a 10.5 × 8.0 km^2 fault plan, that extends between 12 and 19.9 km in depth [20], is associated with the 31 October event.

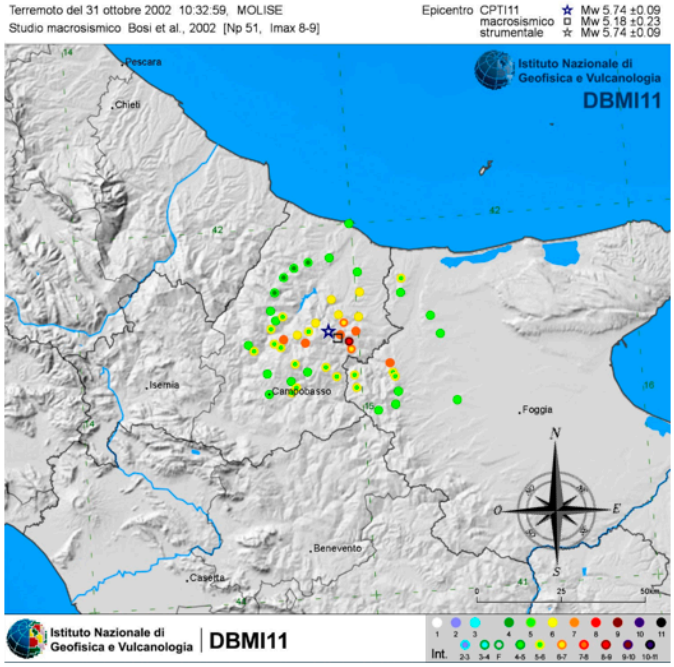

Figure 2. Distribution of earthquake intensities occurring on Thursday, 31 October 2002 [22].

The affected centre falls within a highly seismic zone, which is directly connected to both the Gargano promontory and the Molise Apennine. In this area historical earthquakes with high magnitude (6 and 7) occurred, as shown in Figure 3 [23,24].

From the historical point of view, by means of the Parametric Catalogue of Italian Earthquakes [24], it has been possible to identify the strongest events located near the study area. Particular interest should be given to the spatial distribution of epicentres in the time period between 1456 and 1962. In this time interval the most important events are: the Apennine sequence, which occurred on Sunday, 5 December 1456 (O.S.) (M_w = 7.2, I = XI in the Mercalli-Cancani-Sieberg (MCS) scale), that produced serious damage to the Municipality of Casacalenda; next there was the Garganica sequence of July–September 1627 (M_w = 7.7, I = X in the MCS scale), which caused significant damage in Termoli (I = VIII–IX in the MCS scale) and in Campomarino (I = VIII in the MCS scale); this was followed by the Friday, 26 July 1805 (N.S.) event (M_w = 6.6, I = X in the MCS scale) in the Matese region, whose effects did not exceed the VI MCS in Larino. Referring to the event that occurred on 31 October 2002, the focal mechanism types induced by the mainshocks are strike slip-faults, characterized by vertical fractures with horizontal movements in the E–W and N–S directions and a focal depth of 15–20 km (Figure 4) [23].

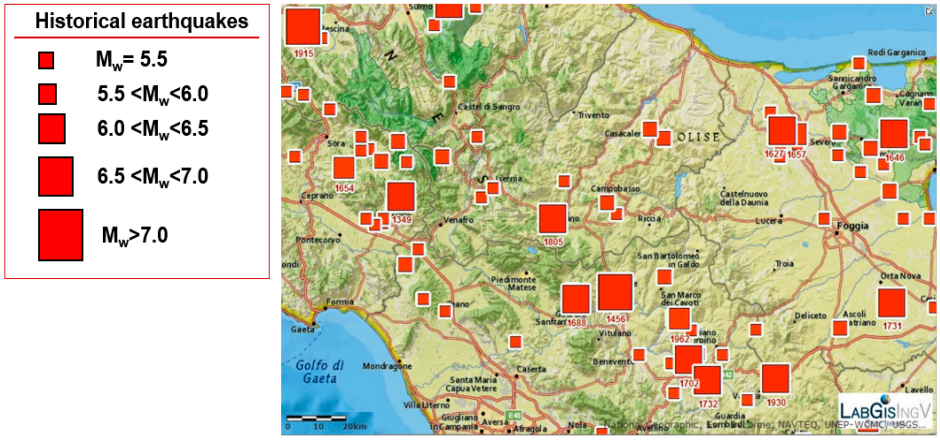

Figure 3. Historical earthquakes in the inspected area [24].

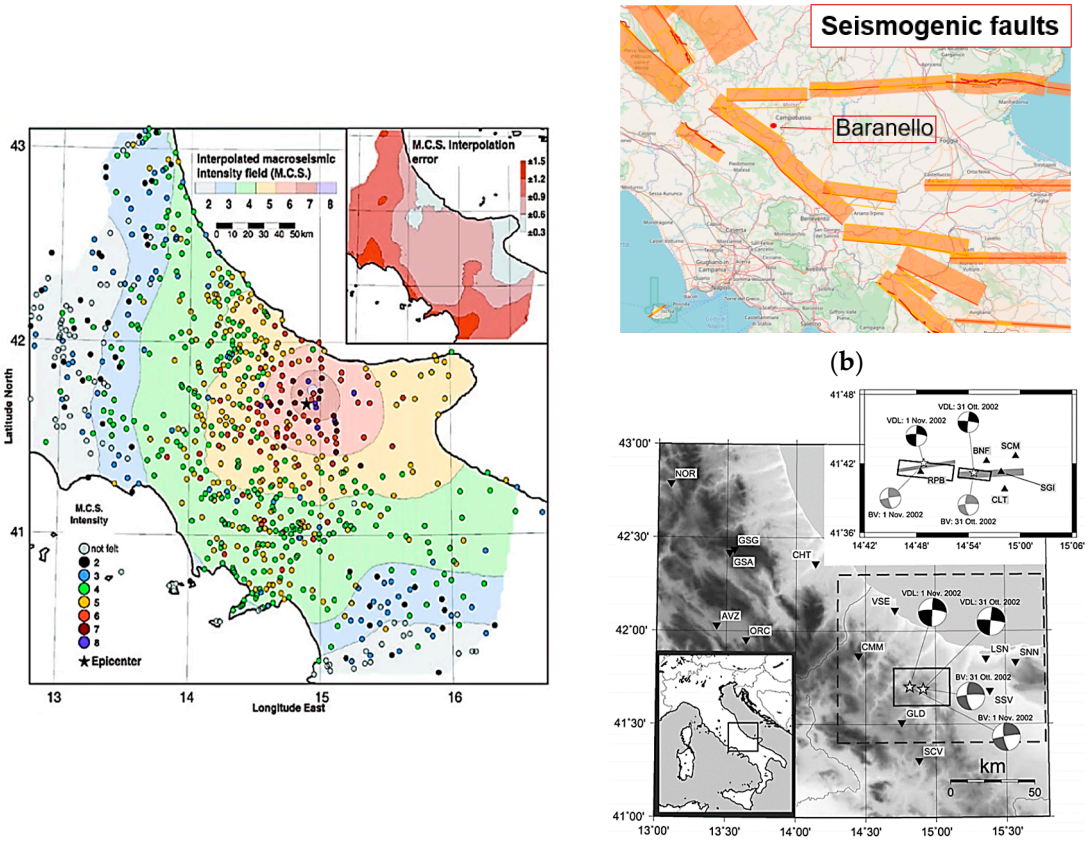

Figure 4. Macroseismic intensities (**a**), seismogenic-faults distribution in the study area (**b**) and focal mechanisms of the fault model (**c**).

Figure 4a shows the macroseismic intensities which occurred after the events previously mentioned. In the area near the epicentre, the maximum intensity recorded was VI according to the MCS scale. Figure 4b illustrates the distribution of the composite seismogenic sources (orange area) based on geological and geophysical data, which are characterized by geometric (strike, dip, width and depth) and kinematic (rake) parameters. Figure 4c describes the surface projections and focal mechanisms of the fault model for the 31 October 2002 Molise earthquakes. Moreover, in the central panel the accelerometric stations (that recorded the mainshocks of the seismic sequence) have been marked with triangles; instead, dashed and solid rectangles point out the stations used to select the source models and the epicentral area [25].

3. Typological and Structural Survey of the Built Area

3.1. The CARTIS Form

The structural and typological characterization is to be considered indispensable for the census of the buildings exposed at risk, which is used for classification purposes into typological classes.

In particular, the CARTIS form has been herein used in order to detect the prevalent ordinary building typologies in municipal or submunicipal territorial parts, called urban sectors, characterized by typological and structural homogeneity.

The CARTIS form has been conceived by the PLINIVS research centre of the University of Naples "Federico II" during the ReLUIS 2014–2016 project "Development of a systematic methodology for the assessment of exposure on a territorial scale based on the typological/structural characteristics of buildings", in collaboration with the Italian Civil Protection Department [26].

The form is divided into four sections: Section 0, for the identification of the municipality and the sectors identified therein; Section 1, for the recognition of each of the relevant typologies characterizing the generic sub-sector of the assigned municipality; Section 2, for the detection of the general characteristics of each typology of constructions; Section 3, for the characterization of structural elements of all individuated construction typologies.

Focusing on the case study, the historical centre of Baranello is composed by one unique compartment, indicated as C01, made of 300 buildings (Figure 5).

From the historical point of view, the analysed municipality is characterized by the presence of construction techniques that over the centuries have maintained their original "asset", dating back to the fourteenth century.

Most of the buildings have been built using rough-hewn stones assembled according to the technique of sack or mixed walls, which in some cases have greatly affected the characteristics and quality of constructions, resulting in substantial deficiencies in terms of global response towards seismic actions.

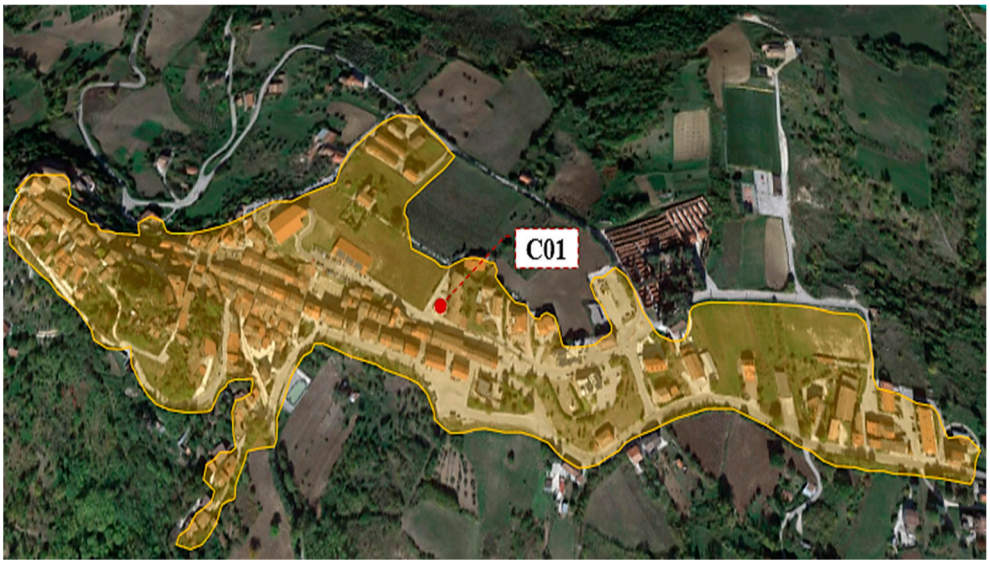

Figure 5. Identification of the urban sector of Baranello.

The houses characterising the historical centre are composed of walls with an average thickness of 0.65 m and an average inter-storey height of 3.50 m. Except for the masonry vaults, the horizontal structures, as well as roofs, are generally made of timber or steel beams (Figure 6).

The data collected through the CARTIS form has allowed, through statistical elaborations, to provide indications on the constructive age, number of storeys, average surface area and wall type of the sample of buildings surveyed within the municipality examined. The results obtained are summarized in the cumulative distributions reported in Figure 7.

Figure 6. Street views of some building typologies inside the inspected historical centre of Baranello.

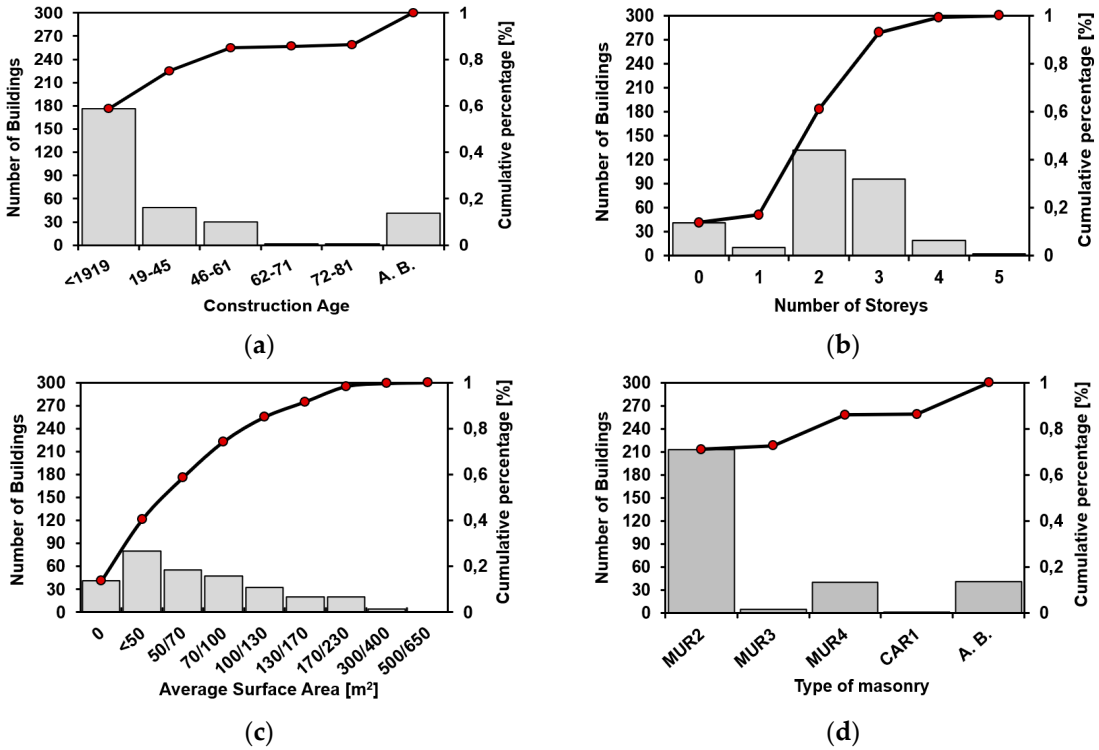

Figure 7. Preliminary characteristics of buildings surveyed in the municipality of Baranello.

From the data surveyed on the 300 inspected buildings, the prevailing typological class is the MUR2 (rough-hewn stone) one, which has been detected in 73% of the cases (220 buildings). Moreover,

the other classes detected in the study area are: MUR3 (rough-hewn masonry stone or pseudo-regular stone, 2% of the sample), MUR4 (regular masonry with squared or brick stones, 13%) and A. B. (unused buildings, 12%).

3.2. The Observed Damage Assessment

Since the 1976 Friuli earthquake (il Terremoto del Friuli, Thursday 6 May 1976 (N.S.)), the investigation of post-earthquake damage to ordinary buildings has become a crucial necessity for emergency management and the recovery phase of Italian historical towns and cities. The visual inspection methods, based upon in situ investigations, have been subjected to substantial changes over time mainly induced by the growth of technical and scientific knowledge in the field of seismic vulnerability.

First of all, the Post-Earthquake Damage and Safety Assessment (AeDES) form was introduced in 1997 as an operational tool, recognized by the Italian Civil Protection Department for the detection and management of post-earthquake emergencies (Figure 8) [27].

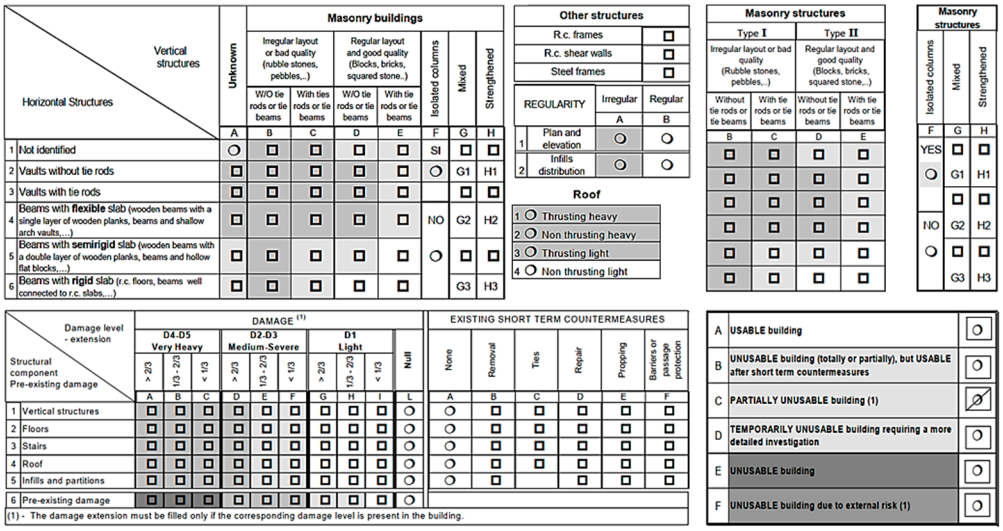

Figure 8. Framework of the main section of the Post-Earthquake Damage and Safety Assessment (AeDES) form.

Subsequently, in 2014, the Italian Civil Protection Department promoted a new scientific project with the aim of creating a new database at the national level to simulate seismic risk scenarios. The project, in collaboration with the Eucentre Foundation (European Centre for the training and research of Earthquake Engineering), led to the development of the Web-GIS platform called Da.D.O (Observed Damage Database) [28].

This tool is of support to the scientific community, since it collects and catalogues the data related to the damages which occurred in the past nine earthquakes (Friuli 1976, Irpinia 1980, Abruzzo 1984, Umbria and Marche 1997, Pollino 1998, Molise and Puglia 2002, Emilia-Romagna 2003, L'Aquila 2009 and Emilia-Romagna 2012), surveyed through the AeDES form, as well as the structural characteristics of inspected buildings.

Thus, for the quantification of the observed damage, using the Da.D.O database and exploiting the information collected in the linked AeDES forms, the Damage Probability Matrices (DPM) have been statistically processed using the binomial distribution function according to the following equation [29]:

$$p_k = \frac{5!}{k!(5-k)!} \times \left(\frac{\mu_D}{5}\right)^k \times \left(1-\frac{\mu_D}{5}\right)^{5-k}, \quad (1)$$

where k denotes the damage threshold variable from 0 to 5 according to the EMS-98 scale and μ_D represents the weighted average of damages.

Moreover, selecting the event which occurred in Molise in 2002, with the epicentre located in Bonefro, it has been possible to deduce the typological classes, the damage levels and the macroseismic intensity of the study area. Subsequently, the graphical representation of DPM has been done, as shown in Figure 9 [28].

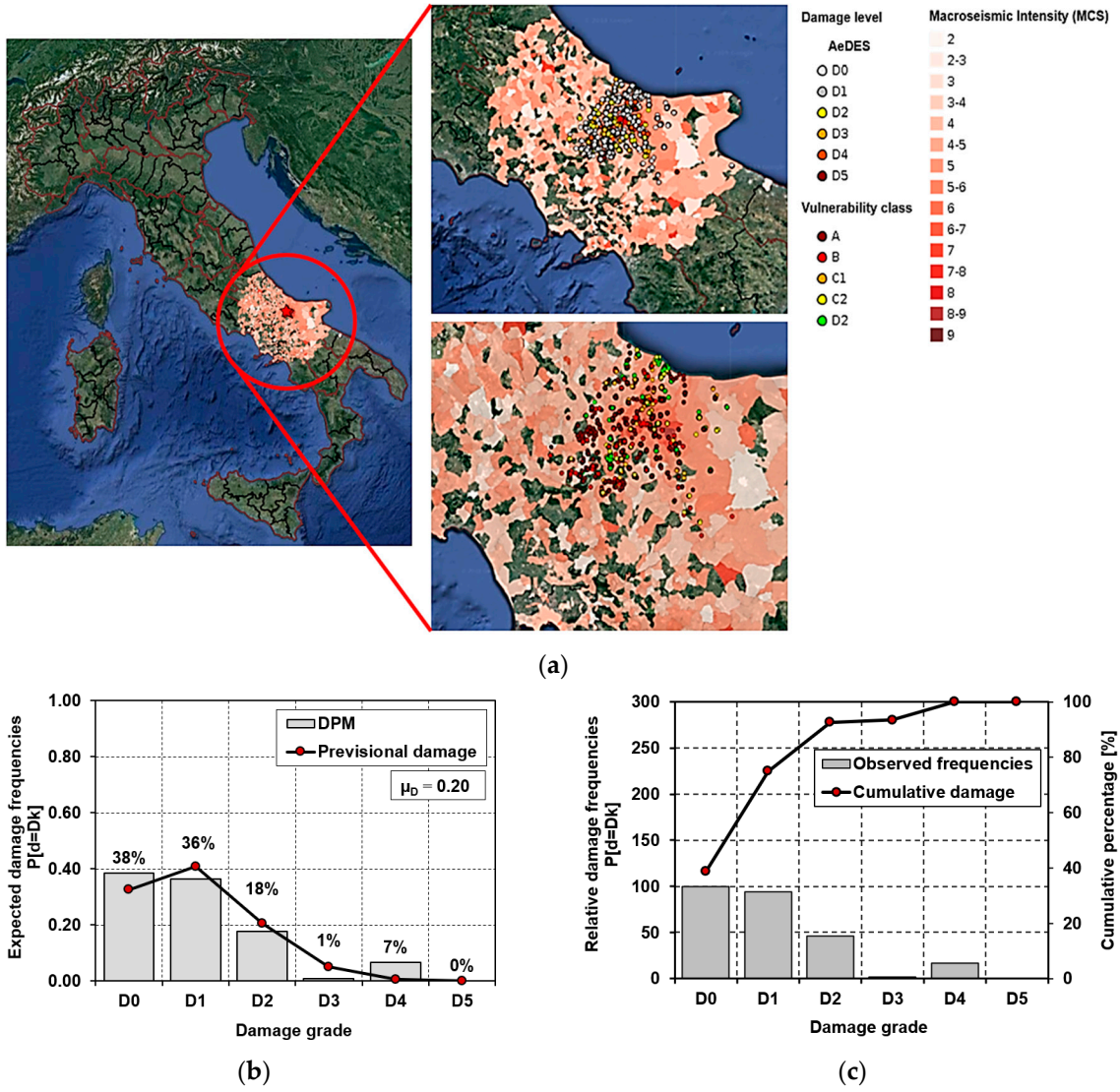

Figure 9. Damage observation: (**a**) Da.D.O database, (**b**) damage probability matrix and (**c**) cumulative damage distribution.

Furthermore, for the typological classification of the surveyed buildings, a parallelism has been conducted between the CARTIS, Da.D.O and EMS-98 methods, as illustrated in Table 1, in order to contextualize the prevalent typological vulnerability classes.

In Table 1, it is noticed that the vulnerability classes are identified on the basis of the vertical structure features. In particular, the compared methods use the vertical structures typologies as a common prerogative for classification purposes, which sees the vulnerability level reduction from MUR1 (irregular stones) masonry buildings to RC framed structures. Likewise, the other methods, which use acronyms or definitions to identify the vertical structure materials, the EMS-98 macroseismic method adopts four classes for their definition from A (the worst) to E (the best).

Table 1. Correlation of vulnerability classes among the CARTIS, Da.D.O and EMS-98 methods.

Typological Vulnerability Classes		
CARTIS	**Da.D.O**	**EMS-98**
MUR 1 Irregular masonry with rounded stones	Irregular Masonry Consisting of shapeless elements (small and medium-sized river pebbles, smoothed and with rounded edges or quarry bachelors) or elements of different sizes with sharp edges, generally in limestone or lava stone.	Masonry with weak or bad quality Rounded or rough-hewn stone masonry of weak or bad quality Class-A Class-B
MUR 2 Irregular masonry with rough stone		
MUR 3 Rough-hewn masonry stone or pseudo-regular stone	Rough masonry Composed of not perfectly squared elements, which appear in pseudo-regular form or with warping stone slabs.	
MUR 4 Regular masonry with squared or brick stones.	Regular masonry Composed of squared elements or solid brick.	Regular masonry stone Class-A Class-B Class-C
CAR 1 RC frame	Other structures RC frame.	Frame structure Class-B Class-D

According to the European Macroseismic Scale (EMS-98), the typological vulnerability classes of the investigated urban area are shown in Figure 10.

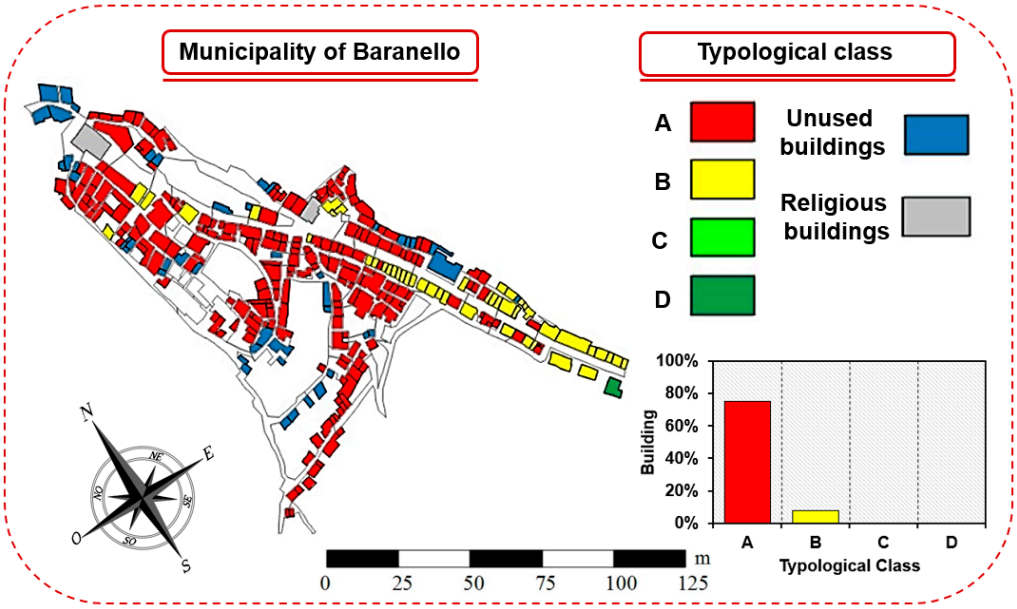

Figure 10. Typological vulnerability classes in the municipality of Baranello.

3.3. Large Scale Seismic Vulnerability Assessment

A seismic vulnerability assessment at the urban scale has been implemented in order to evaluate the propensity for the damage of buildings exposed to earthquakes. In this context, a vulnerability index-based method has been adopted.

The peculiarity of this method, proposed by Formisano et al. (2015) [30] and Formisano et al. (2018) [31], is the possibility of investigating the seismic vulnerability of buildings grouped in compounds through the vulnerability form depicted in Table 2.

Table 2. Vulnerability form for historical clustered buildings.

Parameters	Class Score, S_i				Weight, W_i
	A	**B**	**C**	**D**	
1. Organization of vertical structures	0	5	20	45	1.00
2. Nature of vertical structures	0	5	25	45	0.25
3. Location of the building and the type of foundation	0	5	25	45	0.75
4. Distribution of plan-resisting elements	0	5	25	45	1.50
5. In-plane regularity	0	5	25	45	0.50
6. Vertical regularity	0	5	25	45	0.50
7. Type of floor	0	5	15	45	0.80
8. Roofing	0	15	25	45	0.75
9. Details	0	0	25	45	0.25
10. Physical conditions	0	5	25	45	1.00
11. Presence of an adjacent building with a different height	−20	0	15	45	1.00
12. Position of the building in the aggregate	−45	−25	−15	0	1.50
13. Number of staggered floors	0	15	25	45	0.50
14. Structural or typological heterogeneity among adjacent S.U.	−15	−10	0	45	1.20
15. Percentage difference of opening areas among adjacent facades	−20	0	25	45	1.00

This form, based on the method proposed by Benedetti and Petrini many decades ago [32,33], is appropriate for masonry building aggregates, and uses five new parameters, additional with respect to the original form ten parameters proposed by the above-mentioned researchers, which take into account the effects of mutual interaction under earthquakes among aggregated Structural Units (S.Us). With regard to the five new added parameters, in order to obtain a form totally homogeneous with the previous one, the scores and weights assigned were calibrated numerically on the basis of the results of specific numerical parametric non-linear analyses. These analyses were performed by the 3MURI software, which uses the Frame by the Macro-Elements (FME) computational method. Further information on how scores and classes were determined are found in the aforementioned work by Formisano et al. (2015) [30].

Methodologically, the vulnerability index, I_V, for each S.U., is intended as the weighted sum of the class selected for each of the 15 parameters listed in Table 2 multiplied by the respective weight. The estimated parameters are grouped into four vulnerability classes (A, B, C and D, from the best to the worst), characterised by a specific score (also with a negative sign in case of a vulnerability reduction), to which a correspondent weight, W_i, is assigned, this weight being variable from a minimum of 0.25 for the less important parameters, and up to a maximum of 1.50 for the most important one.

Thus, the vulnerability index, I_V, is calculated according to the following equation:

$$I_V = \sum_{i=1}^{15} S_i \times W_i, \tag{2}$$

where, S_i, are the specific scores associated with each parameter, and W_i are the assigned weights. Subsequently, the vulnerability index value I_V is normalized in the range [0–1] by means of Equation (3), assuming, from this moment, the notation V_I:

$$V_I = \left[\frac{I_V - \left(\sum_{i=1}^{15} S_{min} \times W_i \right)}{\left| \sum_{i=1}^{15} \left[(S_{max} \times W_i) - (S_{min} \times W_i) \right] \right|} \right], \tag{3}$$

where I_V is the vulnerability index deriving from the previously form; $(S_{min} \cdot W_i)$, equal to −125.50, represents the sum of scores associated to the vulnerability class A of each parameter multiplied by respective weights; $(S_{max} \cdot W_i)$, equal to 495.00, represents the sum of scores associated with the

vulnerability class D of each parameter multiplied by the respective weights; and the denominator, equal to 620.50, represents the vulnerability total interval.

According to what has been above specified, the distribution of the typological vulnerability is represented in Figure 11.

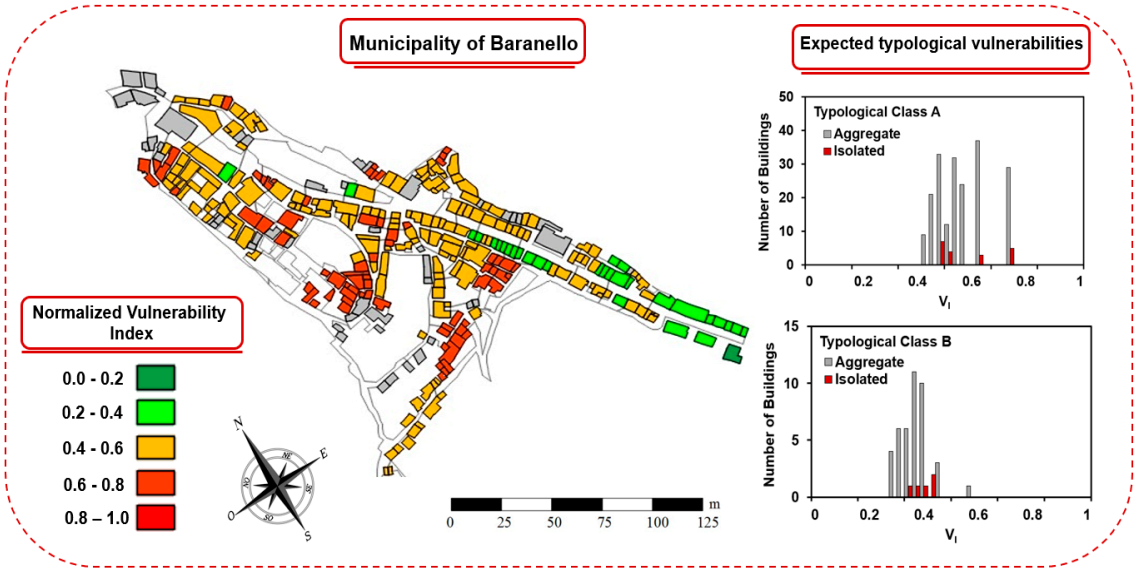

Figure 11. Vulnerability distribution in the municipality of Baranello.

As it is seen in the previous figure, the distribution of the vulnerability results is quite homogeneous, with an expected medium–high vulnerability enclosed in the range [0.4–0.6] for typological class A, while only 30% of the samples have a vulnerability index (V_I) equal to 0.76. Moreover, for the analysed typological class B, the expected frequency is in the range [0.2–0.4], which corresponds to a moderate vulnerability level.

Subsequently, vulnerability curves [34–36] have been obtained to estimate the propensity for the damage of the analysed building stock (Figure 12).

More in detail, these curves express the level of damage achieved as a function of macroseismic intensity "$I_{EMS\text{-}98}$", which is defined according to the European macroseismic scale EMS-98.

In particular, as shown in Equation (4), the vulnerability curves depend upon the vulnerability index (V_I), on the seismic hazard, expressed in terms of macroseismic intensity ($I_{EMS\text{-}98}$) and the ductility factor Q, which describes the ductility of a certain typological class, and assumes, in the case under study, the value of 2.3 [36].

$$\mu_D = 2.5 \times \left[1 + \tanh\left(\frac{I_{EMS\text{-}98} + 6.25 \times V_I - 13.1}{Q}\right)\right] \quad (4)$$

As reported in the previous Figure 12, the vulnerability curves are derived for a sample of buildings representative of the construction types found in the inspected area. However, for a more accurate representation of the expected damage, the mean typological vulnerability curves have been represented together with other curves, taking into account the statistical variability of damage in the vulnerability range ($V_m - \sigma$, $V_m + \sigma$; $V_m + 2\sigma$, $V_m - 2\sigma$) [2,36–38].

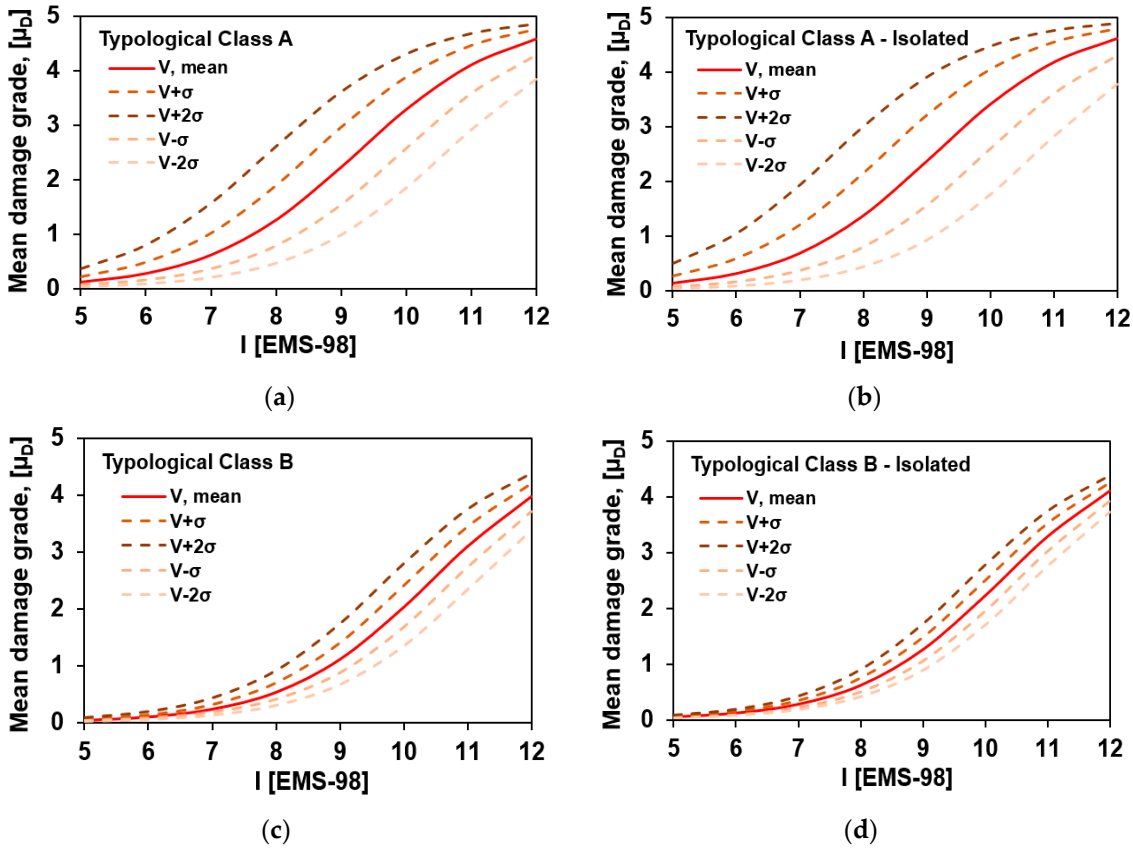

Figure 12. The mean typological vulnerability curves for examined building typologies.

3.4. Estimation of Seismic Impact Scenarios

The evaluation of possible seismic damage scenarios is essential when planning a strategic measure to mitigate the risk. Basically, the earthquake is a natural phenomenon generated by the accumulation of stresses in particular points of the lithosphere, among the surfaces in contact with ancient faults or in other areas. The energy is released under the form of *P*-waves and *S*-waves, which radiate at different velocities in all directions with roughly spherical wavefronts. There is, therefore, an attenuation of the seismic wave energy from the epicentre to the different sites where earthquake effects are felt, since the amplitude of the volume waves decreases according to 1/D (D is the site–source distance), whereas for the surface waves the amplitude decreases about $1/\sqrt{(D)}$.

The prediction of the seismicity of a specific site can be evaluated by adopting appropriate seismic attenuation laws, which are empirical formulations calibrated on the statistical data (instrumental or macroseismic) analysis of earthquakes occurred. Generally, these laws are based on simplified models in order to represent seismic propagation. In practice, an empirical relationship is established between some simple factors (energy released at the source through the magnitude (M_w), distance (D) or hypocentre (h) distances between the epicentre and the site) and some synthetic parameters (a, b, c and d) that better reproduce the set of instrumental or macroseismic observations.

Other research activities [39,40] were conducted to develop attenuation laws, generated in terms of spectral accelerations (S_a) and peak ground accelerations (PGA), or in terms of seismic intensity (MMI), from instrumental recordings of past earthquakes which occurred.

In the current research, the severity of the seismic effects has been analysed by predictive analyses using the following three seismic attenuation laws:

$$I_{EMS\text{-}98} = 6.39 + 1.756 \times M_w - 2.747 \times (R + 7) \quad (5)$$

$$I_{EMS\text{-}98} = 1.0157 + 1.2566 \times M_w - 0.6547 \times \ln\left(\sqrt{R^2 + 2}\right) \quad (6)$$

$$I_{EMS\text{-}98} = 1.45 \times M_w - 2.46 \times \ln(R + 8.16) \quad (7)$$

which were implemented by Crespellani et al. [41], Cauzzi et al. [42] and Esteva and Harris [43], respectively, using the moment magnitude M_w and the site–source distance R (measured in km).

Therefore, the analysis conducted is based on an empirical-forecast method, where the probable damage scenarios are estimated by the disaggregation of the seismic risk obtained combining n-sources. In detail, a deterministic approach has been used by selecting as its reference earthquakes, according to the Parametric Catalogue of Italian Earthquakes (CPTI15) [44], three events of increasing magnitude (4, 5 and 6) having occurred in the past in the Molise Region. After these moment magnitudes have been selected, the definition of different epicentre distances (in the range from 5 to 35 km) has allowed us to plot the expected damage scenarios (Figure 13).

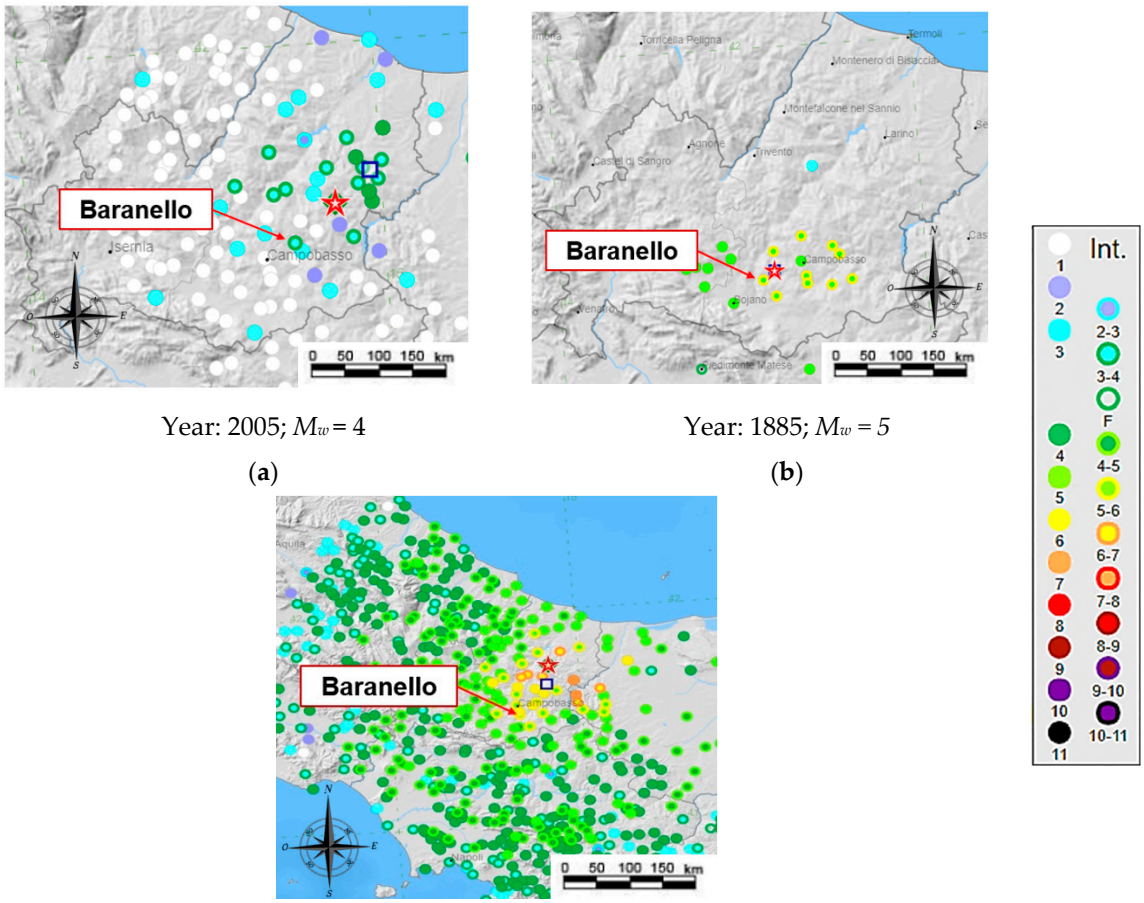

Year: 2005; $M_w = 4$

(**a**)

Year: 1885; $M_w = 5$

(**b**)

Year: 2002; $M_w = 6$

(**c**)

Figure 13. The earthquakes selected for the case study area [43].

In particular, based on the three attenuation laws above mentioned, the macroseismic intensities have been correlated to the earthquake magnitudes on the basis of Equations (5)–(7), leading towards the 27 damage scenarios reported in Table 3.

According to analysis results derived from the previous table, it is possible to notice how the attenuation model proposed by Esteva and Harris [43] is the worst case, since, unlike the other laws, it provides the highest macroseismic intensities. Therefore, the damage scenarios achieved according

to Esteva and Harris' attenuation law considering R = 5 Km have been adopted to represent the most conservative risk assessment case, as shown in Figure 14.

Table 3. The correlation between moment magnitude, M_w, and macroseismic intensity, I_{EMS-98}.

Magnitude M_w	Macroseismic Intensity I_{EMS-98}—Crespellani et al. (1992) [41]		
	R = 5 km	R = 17 km	R = 35 km
4	VII	V	III
5	VIII	VI	V
6	X	VIII	VII
Magnitude M_w	**Macroseismic Intensity I_{EMS-98}—Cauzzi et al. (2008) [42]**		
	R = 5 km	**R = 17 km**	**R = 35 km**
4	V	IV	V
5	VI	VI	V
6	VIII	VII	VII
Magnitude M_w	**Macroseismic Intensity I_{EMS-98}—Esteva and Harris (1970) [43]**		
	R = 5 km	**R = 17 km**	**R = 35 km**
4	X	VII	V
5	XI	VIII	VII
6	XII	X	VIII

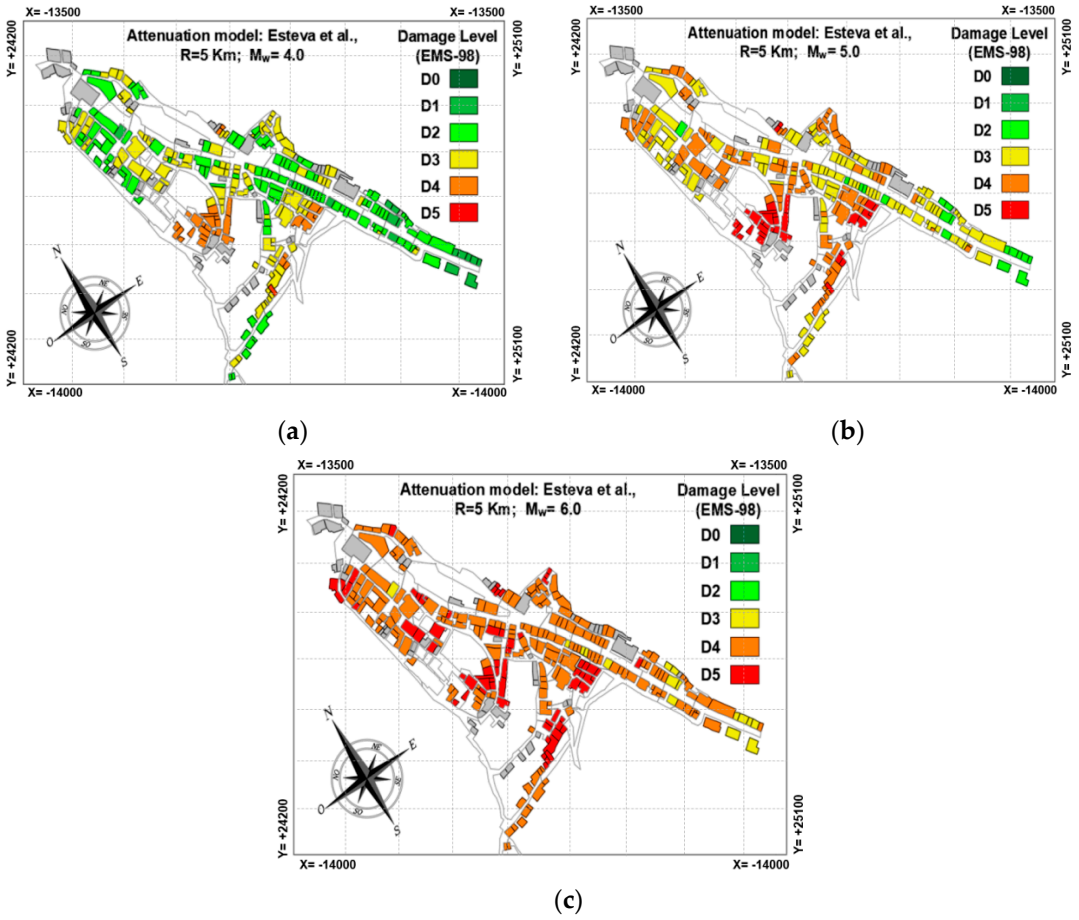

Figure 14. The impact damage scenarios in the investigated urban area (for R = 5 Km and M_w variable from 4 to 6) according to Esteva and Harris' attenuation law.

Then, the correlation between the mean damage grade, μ_D, and the damage thresholds, D_K, have been developed according to the EMS-98 scale (Figure 15) [45,46].

From the analysis results, it appears that for $M_w = 4$ about 61% of the building suffers damage D2, while for $M_w = 6$, damage thresholds D4 (near-collapse) and D5 (collapse) are attained in 68% and 25% of the cases, respectively. Contrarily, when $M_w = 5$, a more variable damage distribution is achieved.

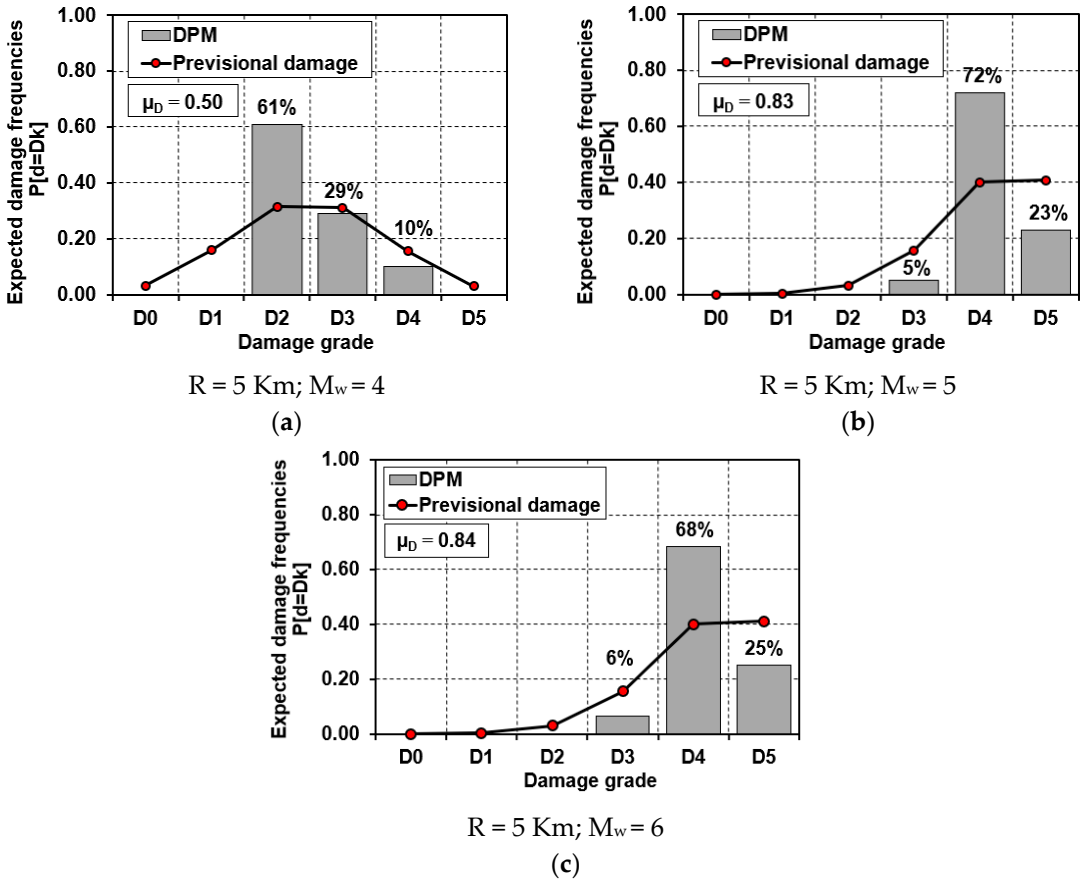

Figure 15. Damage distribution in the urban sector under investigation.

Consequently, having defined the damage distributions, a comparison has been made between the damage obtained through the proposed attenuation models and the corresponding damage achieved from the AeDES survey forms (Figure 16).

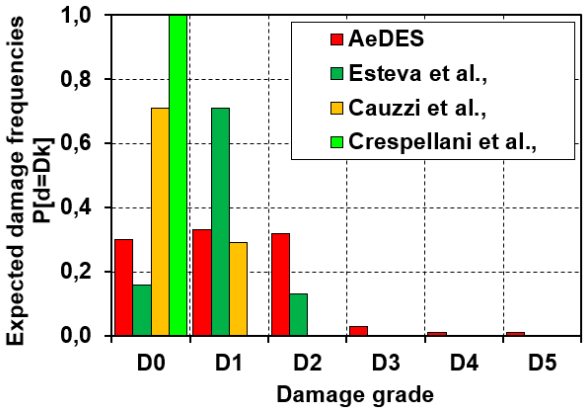

Figure 16. Comparison among damage frequencies in the inspected area between the used attenuation models and the AeDES forms.

From results obtained it is noted that Esteva and Harris' seismic attenuation law [43] allows us to better estimate the damage effectively found on site. Nevertheless, it should be observed that this seismic attenuation law tends to underestimate the damage thresholds D0 and D2, while overestimating the damage level D1.

3.5. Calibration of Typological Vulnerability Curves

Once we applied the vulnerability index methodology, and after having derived the damage scenarios for the whole building stock of the city centre of Baranello, it is possible to calibrate the typological vulnerability curves based on the events which occurred in the examined area.

The proposed method aims at calibrating the typological vulnerability curves based on the macroseismic data collected after the 2002 earthquake. The use of these curves is desirable, since they represent a useful tool for the evaluation of the vulnerability induced by a seismic event through a synthetic parameter, i.e., the mean damage grade (μ_D).

Furthermore, to take into account the variability of seismic motion in terms of macroseismic intensity, using the database Da.D.O, three macroseismic intensity thresholds, recorded after the 2002 Molise earthquake, have been considered. To this purpose, three municipalities of the province of Campobasso have been selected as reference cases. In particular, the municipality of Baranello, with an intensity of V (the starting point of the function), and the cities of San Giuliano di Puglia and Bonefro, with intensity equal to VII and IX, respectively, have been selected, they being considered as homogeneous from typological and structural points of view.

Thus, based on these considerations, a first trial representation of the damage–intensity curve has been provided, as illustrated in Figure 17 [47].

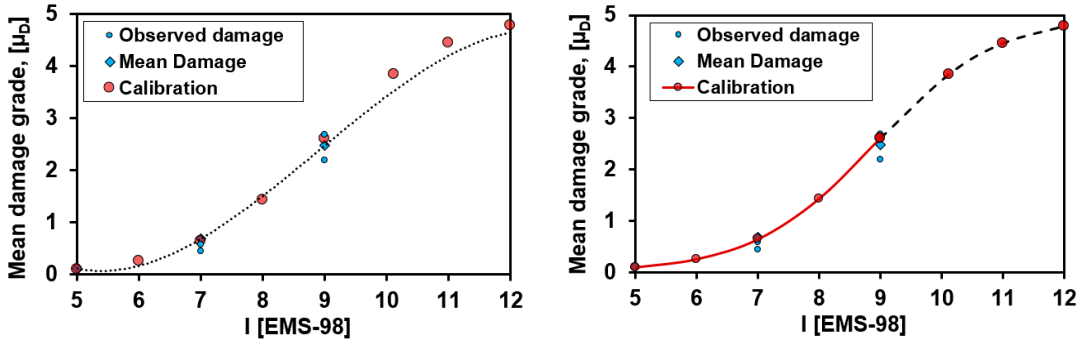

Figure 17. Calibration of vulnerability curves: (**a**) interpolating polynomial function; (**b**) representation of the proposed curve.

Figure 17a shows a third-degree interpolation function able to associate the observed damage grade, achieved by means of the AeDES form, to the mean damage grade, calculated for the V, VII and IX macroseismic intensities. In Figure 17b is shown the mathematical representation of the curve proposed to calibrate the observed damages. In this latter figure, it is worth noting that, since intensities $I_{EMS\text{-}98} > IX$ were not detected in the study area, the curve has a dashed part, corresponding to undetected damages, leading probably towards a threshold damage D5 (collapse).

The mathematic expression of the proposed law is given by the following equation:

$$\mu_D = 2.5 \times \left[1 + \tan h\left(\frac{I_{EMS\text{-}98} + 6.25 \times V_I - \Psi}{Q}\right)\right] \quad (8)$$

where ψ and Q have assumed the values of 12.35 and 2.00 (the latter analogous to the ductility factor suggested by Eurocode 8 for masonry buildings), respectively, in order to have the mathematical (red) curve perfectly superimposable to the third-degree interpolation relationship.

Finally, Figure 18 shows the comparison between the proposed curve and that deriving from the method presented by Lagomarsino and Giovinazzi [34] for the typological classes A and B, which are characterised by an average vulnerability index of 0.55 and 0.34, respectively.

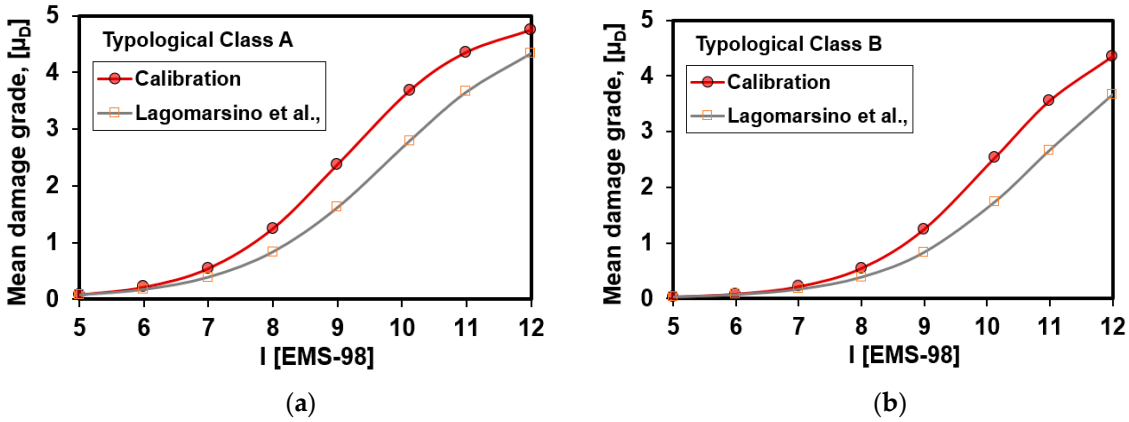

Figure 18. Comparison between the proposed curves and those derived from the macroseismic method proposed by Lagomarsino (2006) [33] for typological classes A and B.

It can be seen how the proposed curve provides expected damage values higher than the ones derived from the other method, which is based on the empirical–mechanical procedure developed in the framework of the Risk-UE project for different samples of buildings belonging to several European Countries. In particular, for Class A buildings, the proposed formulation provides, for macroseismic intensities V, VII and IX, damage percentage increases equal to 12%, 41% and 46%, respectively, in comparison to those foreseen by Lagomarsino. On the other hand, for Class B buildings these increments, corresponding to macroseismic intensities VII and IX only, are equal to 26% and 48%, respectively.

Definitely, from the above Table 4, it appears that the proposed formulation, if compared to the Lagomarsino and Giovinazzi method, provides results on the safe side in predicting the possible expected damages in the examined area.

Table 4. Comparison in terms of mean damage grades between the proposed formulation results and Lagomarsino and Giovinazzi's relationship ones for the macroseismic intensities recorded in the investigated area.

Analysis Method and Typological Class	Mean Damage Grade, μ_D		
	V	VII	IX
Lagomarsino and Giovinazzi (2006) [34]—Class A	0.072	0.38	1.61
Calibrated curve—Class A	0.081	0.54	2.37
Damage increment	12%	41%	46%
Lagomarsino and Giovinazzi (2006) [34]—Class B	0.030	0.16	0.83
Calibrated curve—Class B	0.030	0.21	1.24
Damage increment	-	26%	48%

4. Influence of the Geological Conditions on the Ground Motion

4.1. Local Site Effects

In the framework of large-scale vulnerability analysis, the evaluation of site effects plays a fundamental role for a correct prediction of the expected damage, and therefore, to implement suitable risk mitigation measures to safeguard people's life and to preserve the integrity of historical heritage constructions.

From the physical point of view, the local seismic response can be intended as a set of changes in amplitude, duration and frequency content that a seismic motion, relative to a bedrock basement, undergoes through the overlying layers of soil up to the surface. In other words, the ground layers can increase the amplitude of the seismic motion at some frequencies and reduce it for other ones.

The schematization of seismic motion can be represented both in the domain of time and frequencies. In particular, considering the time domain, the parameters most frequently used to describe the earthquake characteristics are the peak value of the acceleration, the velocity, the displacements, and finally, the duration. In the second case (frequency domain), the parameters of seismic motion are characterized by either the Fourier spectrum or the response spectrum. The quantitative evaluation of the local seismic response can, therefore, be carried out on the basis of the comparison between different quantities representative of the surface seismic motion and the reference one (bedrock).

The problem of geo-hazard effects has been already contemplated by two works of Chieffo and Formisano (both 2019) [18,48], where, under a macroseismic approach, and on the basis of macroelement numerical analysis on clustered buildings, the site effects were taken into account through a local amplification coefficient, f_{PGA}, defined as the ratio between the maximum recorded acceleration at the ground surface ($a_{max,s}$) and that at the bedrock ($a_{max,r}$), as reported in Equation (9).

$$f_{PGA} = \frac{a_{max,s}}{a_{max,r}} \quad (9)$$

4.2. Geological Conditions of the Study Area

Focusing on the case study, the historic centre area of Baranello is characterized by a geological structure mainly derived from covering tectonics related to the formation of the Apennine chain and sub-Apennine reliefs.

The sedimentary series, variously displaced and dismembered, were poured into the Molise basin causing anomalous overlaps and outcropping of very different units both for facies and for age and paleogeographic genesis.

The territory is characterised by the presence of a heterogeneous soil constituted by a basal interval formed in large part by outcrops found along the middle-basal bands of the local slopes. Two lithofacies have been distinguished. The first, namely the dominant pelitic–flysch of St. Bartolomeo, is characterized by a cohesive behaviour type, represented by silt–sand clays and clay–silt marls of different colours, from gray–blue to brown, with sporadic intercalations of a calcareous and arenaceous nature. The clayey lithotypes are characterized by a modest technical quality, that tends to significantly reduce in the superficial layers more exposed to exogenous degradation, and in particular, to the erosive and plasticizing action produced by the corrosive and infiltration waters. The resistance characteristics are, therefore, globally linked to the clay component, and under the conditions of short-term periods, they are essentially regulated by the undrained cohesion parameter. Moreover, the permeability degree could be considered practically null, since there is no interstitial water circulation. On the other hand, the second lithofacies, mainly made of stones, are due to an irregularly stratified marly–limestone–arenaceous succession, in which layers of limestones and coarse sandstones are identified with centimetric alternations of arenaceous and silt–marly levels and dense, stratified, clay–silt layers.

Finally, the formations described previously are generally surmounted by extensive coverings of both secondary genesis and areal thickness, represented essentially by colluvial deposits or by the localized accumulations of carryovers, whose presence is substantially connected to the local infrastructural development of the area.

For the seismic microzonation of this historic centre, data from in situ surveys made available by the Municipal Administration of Baranello are used. Furthermore, in situ tests were carried out to identify the stratigraphy. Figure 19 shows the areas where the Down-Hole geological characterization tests were carried out. These tests provide the velocity of the propagation of seismic waves, compression and shear, at different depths.

Thus, measuring the time these waves go from the source (on the surface) to the receiver (located inside a properly prepared hole), it is possible to derive the parameters of the soils traversed.

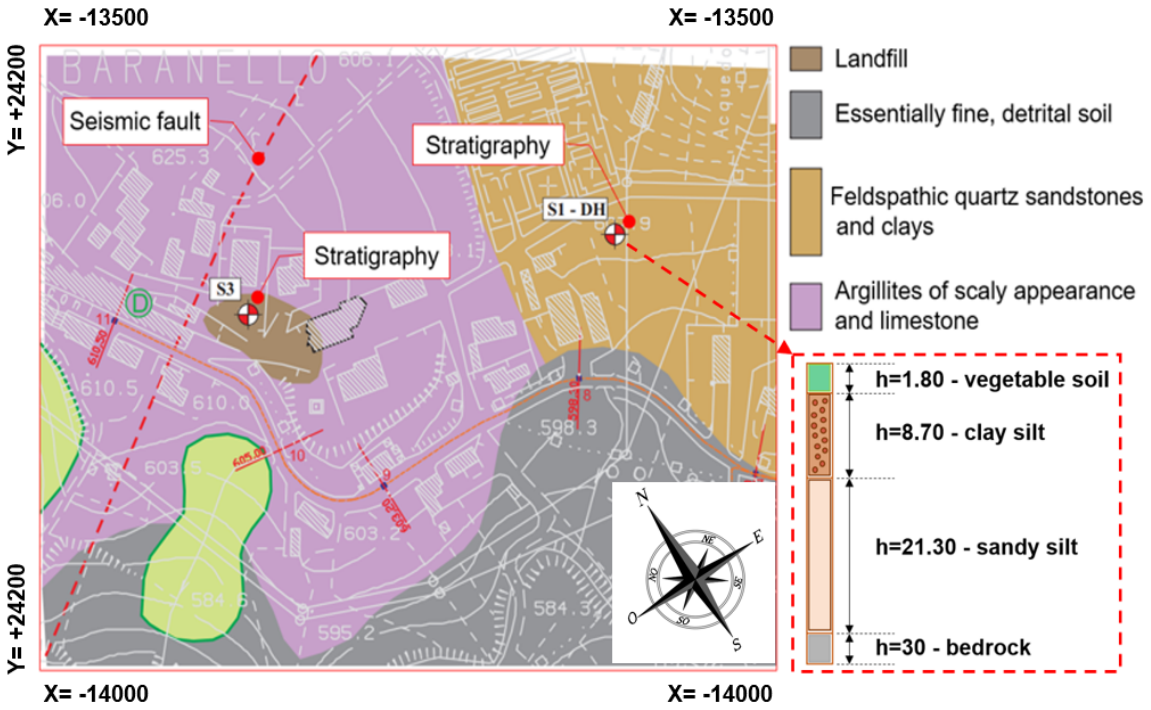

Figure 19. The identification of the in situ geological tests.

The positions of tests, indicated with S1 and S3 in Figure 19, give back the ground stratigraphy consisting of deposits of clay silt and silty sand with a bedrock basement located at 30 m of depth. The seismic subsoil category associated with this ground type is the B one according to the Italian technical standard NTC18 [49].

4.3. Evaluation of the Geological Amplification Factor

The evaluation of the local amplification coefficient has been estimated according to a time domain, since the main purpose of the work is to characterize the maximum ground amplification deriving from local site effects to correctly predict damage scenarios. Therefore, the accelerogram of the event which occurred in Molise in 2002 with its epicentre located in Bonefro. has been used. The event was characterized by a magnitude, M_w, equal to 6 with a maximum PGA = 0.55 g.

To this purpose, STRATA 1.0 software [50], developed at the University of Texas, was used for simplified 1D numerical modelling of the geological conditions of seismic motion at bedrock. More precisely, noting the accelerogram at the crustal surfaces, it is possible to "transport" the seismic input to the bedrock. In this case, once the soil stratigraphy is defined, the software implicitly takes into account the "filter" effect of the soil layers.

The evaluation of the local seismic amplification factor, therefore, provides a clear and effective representation of the filtering effect of a soil deposit on seismic waves. Thus, based on these considerations, starting from the accelerogram recorded after the Molise earthquake, in Figure 20 the accelerogram at the bedrock and the corresponding amplified on the crustal-surface have been derived and graphically depicted.

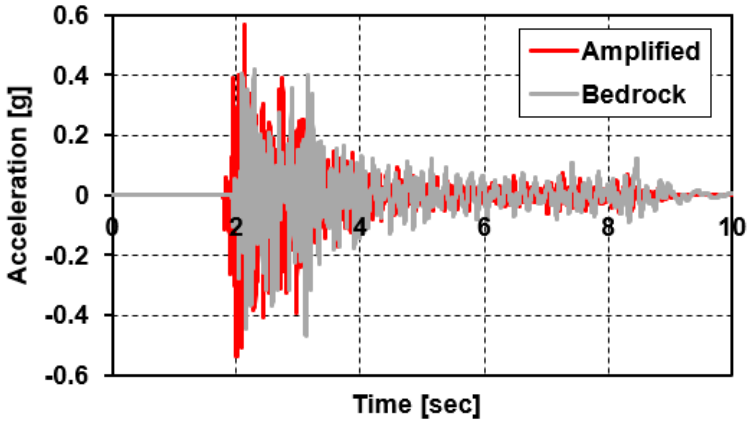

Figure 20. The elaborated accelerograms.

As it is seen in the previous figure, local site effects provide an increase of accelerations detected at the bedrock. In particular, the amplification factor f_{PGA} computed according to Equation (9) provides the results illustrated in Table 5.

Table 5. Amplification factor based on time domain.

Time History	Acceleration [g]		
	Amplified—$a_{max,s}$	**Bedrock—$a_{max,r}$**	**f_{PGA}**
10 s	0.56	0.42	1.33

In the presented table, the recorded amplification coefficient is equal to 1.33, which means that the increment of the seismic motion from the bedrock basement to the crustal surface is equal to 33%.

From these obtained results, and depending on the geologic conditions detected for the case study area, the mean damage degree, μ_D, of the investigated structural units determined in Section 3.3 can be amplified by the above f_{PGA} factor, leading to a more correct expected damage grade $\mu_{D,s}$ [43]:

$$\mu_{D,s} = \mu_D \times f_{PGA} \quad (10)$$

Finally, a synthetic representation of the new damages achieved has been shown in Figure 21 for the already considered combinations of magnitudes and site–source distances.

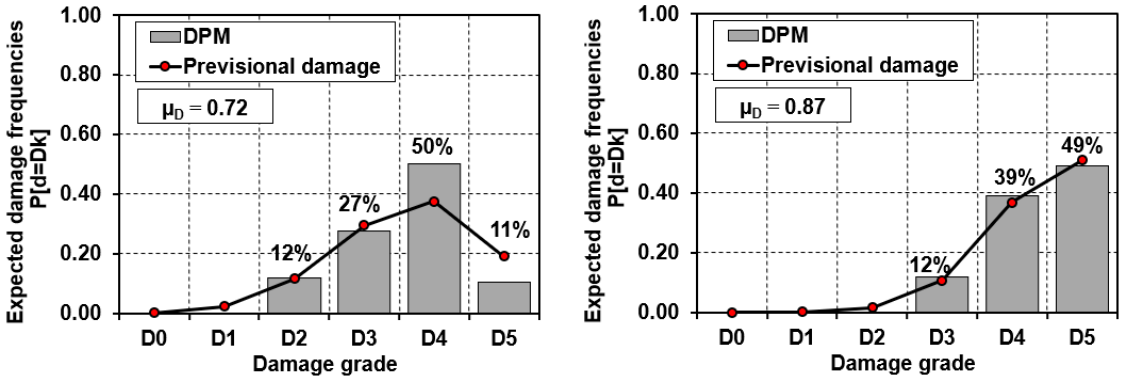

R = 5 Km; M_w = 4 (**a**) R = 5 Km; M_w = 5 (**b**)

Figure 21. *Cont.*

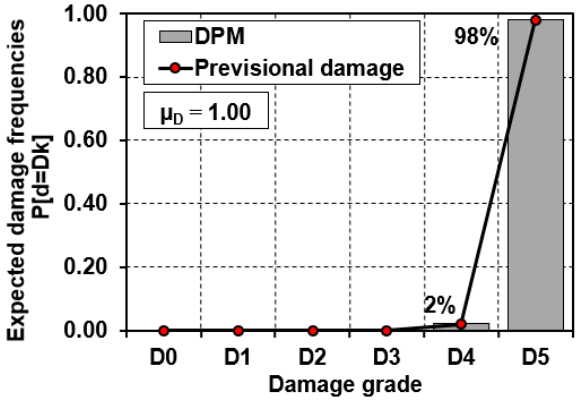

R = 5 Km; M w = 6

(**c**)

Figure 21. Damage distribution considering local seismic amplification effects.

Comparing the new damage scenario to that reported in Section 3.4 (Figure 15), it is possible to estimate the damage increase due to site effects, as reported in Figure 22.

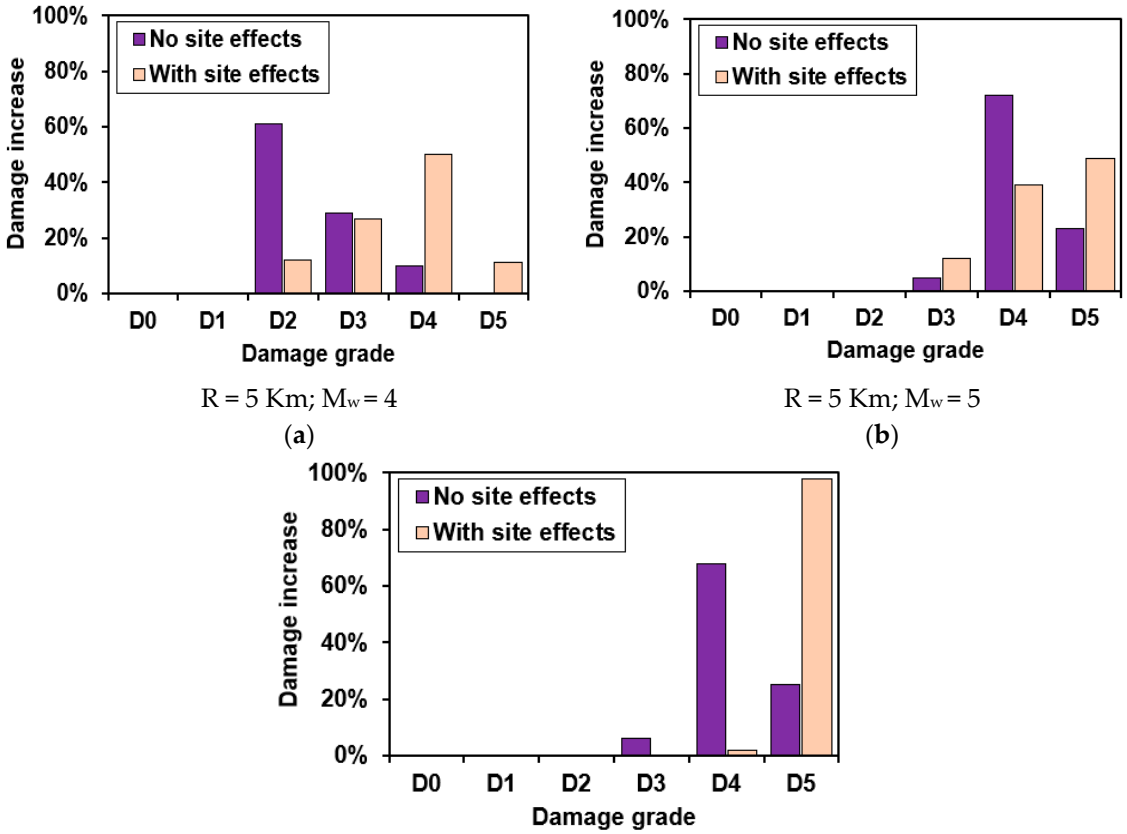

R = 5 Km; Mw = 4

(**a**)

R = 5 Km; Mw = 5

(**b**)

R = 5 Km; M w = 6

(**c**)

Figure 22. The damage scenarios with and without local seismic effects: comparison of results.

As observed in the above figure, the local site effects produce a very high increase of the expected damage. In particular, it is noted that, for an epicentre distance of 5 km, the damage distribution tends to increase towards higher levels of damage. This result is much more evident when M_w = 6 is considered, since the D4 damage level is drastically reduced, while the D5 one is strongly increased.

5. Concluding Remarks

This study proposes a simplified methodology to analyse the seismic vulnerability of masonry building aggregates located in historic centres considering the influence of geo-hazard conditions. An urban sector of 300 buildings in the historical centre of Baranello, in the district of Campobasso (Italy), has been identified as study area for the application of the proposed analysis method.

Firstly, the characterisation of the typological classes of the urban sector examined has been done by means of the CARTIS form, which has allowed us to classify the building compounds from the structural point of view. From on-site recognition, it has been detected that the prevailing typological class of masonry buildings is the MUR2 (rough-stone) one, which represents 75% of the building stock examined. Timber or steel beams and masonry vaults have been detected in the inspected buildings as the main horizontal structures. For the quantification of the observed damage, the AeDES formed conjunctly with the Da.D.O database have been adopted to statistically derive the damage probability matrices. The gotten results have shown that 38% of the buildings have damage D0 (null), while 36% of them reached a damage level D1 (negligible to slight damage).

Subsequently, the seismic vulnerability of the inspected urban sector has been estimated through a vulnerability index method conceived for building aggregates. In the urban area, two distinct typological classes, namely A and B, have been identified according to the EMS-98 scale. It is worth noting that the distribution of vulnerability results for typological class A is quite homogeneous, with an expected medium-high vulnerability enclosed in the range [0.4–0.6], while only 30% of the building sample has a vulnerability index equal to 0.76. Contrarily, for the analysed typological class B, the expected frequency is in the range [0.2–0.4], which corresponds to a moderate vulnerability level.

The damage scenarios of the investigated urban sector, based on a specific seismic attenuation law, have been estimated for different moment magnitudes and site–source distances. The results obtained have shown how Esteva and Harris' attenuation model, if compared to the other attenuation laws, provides the most unfavourable condition in terms of expected damage. In fact, from the statistical processing of expected damages for a moment magnitude equal to 6, a damage threshold D4 (near-collapse) has been attained in 68% of the cases, whereas only 25% of buildings has reached a damage D5 (collapse).

Furthermore, once the damage scenarios have been derived for the whole building stock, the typological vulnerability curves, based on the macroseismic data collected after the 2002 earthquake, have been calibrated on the basis of the seismic damages detected in the examined area. More in detail, three hazard-levels expressed in terms of macroseismic intensity have been considered. In particular, according to the Molise seismic event which occurred in 2002, for the Municipality of Baranello an intensity of V has been considered, whereas for the cities of San Giuliano di Puglia and Bonefro the intensities recorded have been VII and IX, respectively. Thus, the classical formulation of the mean damage grade has been slightly modified in order to calibrate the experimental evidences in terms of damage. To this purpose, a value equal to 12.35 has been associated with the coefficient ψ, that affects the slope of the curve, whereas the ductility factor, Q, has been assumed equal to 2, according to the provisions of Eurocode 8 for masonry buildings. Considering the typological class, A, the proposed curve provides, considering the aforementioned hazard thresholds, a damage percentage increase of 12%, 41% and 46% for seismic intensities V, VII and IX, respectively. On the other hand, the class B buildings have damage increments of 26% and 48% for seismic intensities VII and IX, respectively.

Finally, a local seismic amplification factor has been defined according to the time-domain method. To this purpose, a simplified 1D numerical modelling of the geological conditions of seismic motion has been considered. More precisely, noting the accelerogram at the crustal surfaces, it has been possible to "transport" the seismic input to the bedrock. In this case, once the soil stratigraphy has been defined, the used software implicitly has taken into account the "filter" effect of the soil layers. The evaluation of the local seismic amplification factor has, therefore, provided a clear and effective representation of the filtering effect of soil deposits on seismic waves.

Looking at the analysis results, the esteemed amplification factor has been found as equal to 1.33, which means that the seismic motion increment from the bedrock basement to the crustal surface is equal to 33%. From the new damage scenarios considering local effects, it has been detected as a considerable damage increment. In particular, it has been noted that for the epicentre distance of 5 km and moment magnitude of 4, damage thresholds D2 and D3 have been attained with a damage occurrence probability less than that of the basic case in which the soil influence has been neglected. Contrary to this, the D4 and D5 damage levels significantly increase due to the site effects. On the other hand, considering the worst scenario (R = 5 km and M_w = 6), the site effects have reduced drastically the damage levels D3 and D4, but they have increased the D5 threshold with the collapse of 98% of the buildings in the analysed area.

In conclusion, the proposed work has represented an important starting point for large-scale vulnerability and risk analysis considering site effects, so providing a comprehensive method to predict more precisely damage scenarios into historical centres. In this context, the applicability and feasibility of the proposed research can be considered extendable also to other seismic regions characterized by different types of masonry buildings. To this purpose, the characterization of the sample of buildings is an essential tool for large-scale analysis, since it allows us to evaluate the distribution and frequency of expected vulnerabilities.

This issue is of fundamental importance, since the proposed approach, which will allow us to take into account in a simplified way the influence of site effects on the overall response of buildings, can be used for planning effective seismic risk mitigation interventions.

Author Contributions: Methodology, A.F.; Investigation, N.C.; Data Curation, N.C. and A.F.; Writing-Original Draft Preparation, N.C.; Writing-Review & Editing, A.F. All authors have read and agreed to the published version of the manuscript.

Funding: This research did not receive any external funding.

Acknowledgments: The authors would like to acknowledge the Vice Mayor Domenico Boccia for the interest demonstrated towards the present study, the Surveyor Gianni Caruso for his profuse availability during the site-inspections and Eng. Umberto Capriglione of the Regional Civil Protection Department for providing the macroseismic data of the 2002 earthquake. Also, the financial support given by the WP2 Cartis "Inventory of existing structural and building types" research line of the DPC-ReLUIS 2019-2021 project, where the current research activity was developed, is gratefully acknowledged.

Conflicts of Interest: The authors declare no conflict of interest.

References

1. Ferreira, T.M.; Maio, R.; Vicente, R. Seismic vulnerability assessment of the old city centre of Horta, Azores: calibration and application of a seismic vulnerability index method. *Bull. Earthq. Eng.* **2017**, *15*, 2879–2899. [CrossRef]
2. Chieffo, N.; Formisano, A.; Ferreira, T.M. Damage scenario-based approach and retrofitting strategies for seismic risk mitigation: an application to the historical Centre of Sant'Antimo (Italy). *Eur. J. Environ. Civ. Eng.* **2019**. [CrossRef]
3. Gonzalez-Drigo, R.; Avila-Haro, A.; Barbat, A.H.; Pujades, L.G.; Vargas, Y.F.; Lagomarsino, S.; Cattari, S. Modernist unreinforced masonry (URM) buildings of barcelona: Seismic vulnerability and risk assessment. *Int. J. Archit. Herit.* **2015**, *9*, 214–230. [CrossRef]
4. Calvi, G.M.; Pinho, R.; Magenes, G.; Bommer, J.J.; Restrepo-Vélez, L.F.; Crowley, H. Development of seismic vulnerability assessment methodologies over the past 30 years. *ISET J. Earthq. Technol.* **2006**, *43*, 75–104.
5. Dolce, M.; Kappos, A.; Masi, A.; Penelis, G.; Vona, M. Vulnerability assessment and earthquake damage scenarios of the building stock of Potenza (Southern Italy) using Italian and Greek methodologies. *Eng. Struct.* **2006**, *28*, 357–371. [CrossRef]
6. Clementi, F.; Gazzani, V.; Poiani, M.; Lenci, S. Assessment of seismic behaviour of heritage masonry buildings using numerical modelling. *J. Build. Eng.* **2016**, *8*, 29–47. [CrossRef]

7. Cacace, F.; Zuccaro, G.; De Gregorio, D.; Perelli, F.L. Building Inventory at National scale by evaluation of seismic vulnerability classes distribution based on Census data analysis: BINC procedure. *Int. J. Disaster Risk Reduct.* **2018**, *28*, 384–393. [CrossRef]
8. Cara, S.; Aprile, A.; Pelà, L.; Roca, P. Seismic Risk Assessment and Mitigation at Emergency Limit Condition of Historical Buildings along Strategic Urban Roadways. Application to the "Antiga Esquerra de L'Eixample" Neighborhood of Barcelona. *Int. J. Archit. Herit.* **2018**, *12*, 1055–1075. [CrossRef]
9. Formisano, A. Theoretical and Numerical Seismic Analysis of Masonry Building Aggregates: Case Studies in San Pio Delle Camere (L'Aquila, Italy). *J. Earthq. Eng.* **2017**, *21*, 227–245. [CrossRef]
10. Vicente, R.; Ferreira, T.M.; Maio, R. Seismic Risk at the Urban Scale: Assessment, Mapping and Planning. *Procedia Econ. Financ.* **2014**, *18*, 71–80. [CrossRef]
11. Maio, R.; Ferreira, T.M.; Vicente, R.; Estêvão, J. Seismic vulnerability assessment of historical urban centres: Case study of the old city centre of Faro, Portugal. *J. Risk Res.* **2016**, *19*, 551–580. [CrossRef]
12. Di Pasquale, G.; Orsini, G.; Romeo, R.W. New developments in seismic risk assessment in Italy. *Bull. Earthq. Eng.* **2005**, *3*, 101–128. [CrossRef]
13. Miranda, E.; Hesameddin, A. *Probabilistic Response Assessment for Building-Specific Loss Estimation Building-Specific Loss Estimation*; Pacific Earthquake Engineering Research Center: Berkeley, CA, USA, 2003; pp. 1–60.
14. Baker, J.W.; Cornell, C.A. Uncertainty propagation in probabilistic seismic loss estimation. *Struct. Saf.* **2008**, *30*, 236–252. [CrossRef]
15. Giovinazzi, S. Geotechnical hazard representation for seismic risk analysis. *Bull. N. Z. Soc. Earthq. Eng.* **2009**, *42*, 308. [CrossRef]
16. Lanzo, G.; Silvestri, F.; Costanzo, A.; d'Onofrio, A.; Martelli, L.; Pagliaroli, A.; Sica, S.; Simonelli, A. Site response studies and seismic microzoning in the Middle Aterno valley (L'aquila, Central Italy). *Bull. Earthq. Eng.* **2011**, *9*, 1417–1442. [CrossRef]
17. Suwal, S.; Pagliaroli, A.; Lanzo, G. Comparative Study of 1D Codes for Site Response Analyses. *Int. J. Landslide Environ.* **2014**, *2*, 24–31.
18. Chieffo, N.; Formisano, A. The influence of geo-hazard effects on the physical vulnerability assessment of the built heritage: An application in a district of Naples. *Buildings* **2019**, *9*, 26. [CrossRef]
19. Viaggio Molise (n.d.). Available online: https://www.viaggiomolise.it/baranello/ (accessed on 10 July 2019). (In Italian).
20. Valensise, G.; Pantosti, D.; Basili, R. Seismology and tectonic setting of the 2002 Molise, Italy, earthquake. *Earthq. Spectra* **2004**, *20*. [CrossRef]
21. Morasca, P.; Zolezzi, F.; Spallarossa, D.; Luzi, L. Ground motion models for the Molise region (Southern Italy). *Soil Dyn. Earthq. Eng.* **2008**, *28*, 198–211. [CrossRef]
22. National Institute of Geophysics and Volcanology (INGV), Database Macrosismico Italiano (DBMI11), (n.d.). Available online: https://emidius.mi.ingv.it/DBMI11/ (accessed on 22 July 2019). (In Italian).
23. Giuliani, R.; Anzidei, M.; Bonci, L.; Calcaterra, S.; D'Agostino, N.; Mattone, M.; Pietrantonio, G.; Riguzzi, F.; Selvaggi, G. Co-seismic displacements associated to the Molise (Southern Italy) earthquake sequence of October-November 2002 inferred from GPS measurements. *Tectonophysics* **2007**, *432*, 21–35. [CrossRef]
24. National Institute of Geophysics and Volcanology (INGV), LabGIS, (n.d.). Available online: http://www.gm.ingv.it/index.php/labgis?jjj=1566641830525 (accessed on 22 July 2019). (In Italian).
25. Vallèe, M.; Di Luccio, F. Source analysis of the 2002 Molise, southern Italy, twin earthquakes (10/31 and 11/01). *Geophys. Res. Lett.* **2005**, *32*, 1–4. [CrossRef]
26. Zuccaro, G.; Della Bella, M.; Papa, F. Caratterizzazione tipologico strutturali a scala nazionale. In Proceedings of the 9th National Conference ANIDIS, l'Ingegneria Sismica, Italy, 20–23 September 1999. (In Italian).
27. Baggio, C.; Bernardini, A.; Colozza, R.; Corazza, L.; Della Bella, M.; Di Pasquale, G.; Dolce, M.; Goretti, A.; Martinelli, A.; Orsini, G.; et al. Manuale per la Compilazione Della Scheda di Primo Livello di Rilevamento Danno, Pronto Intervento e Agibilità per Edifici Ordinari Nell'emergenza Post-Sismica (AeDES), 2009, 113. Available online: http://www.protezionecivile.gov.it/media-comunicazione/pubblicazioni/dettaglio/-/asset_publisher/default/content/manuale-per-la-compilazione-della-scheda-di-1-livello-di-rilevamento-di-danno-pronto-intervento-e-agibilita-per-edifici-ordinari-nell-emergenza-post-s (accessed on 22 July 2019). (In Italian)

28. European Centre for Training and Research in Earthquake Engineering, Database di Danno Osservato (Da.D.O), (n.d.). Available online: http://egeos.eucentre.it/danno_osservato/web/danno_osservato# (accessed on 22 July 2019). (In Italian).
29. Rapone, D.; Brando, G.; Spacone, E.; De Matteis, G. Seismic vulnerability assessment of historic centers: description of a predictive method and application to the case study of scanno (Abruzzi, Italy). *Int. J. Archit. Herit.* **2018**, *12*, 1171–1195. [CrossRef]
30. Formisano, A.; Florio, G.; Landolfo, R.; Mazzolani, F.M. Numerical calibration of an easy method for seismic behaviour assessment on large scale of masonry building aggregates. *Adv. Eng. Softw.* **2015**, *80*, 116–138. [CrossRef]
31. Formisano, A.; Chieffo, N.; Mosoarca, M. Seismic Vulnerability and Damage Speedy Estimation of an Urban Sector within the Municipality of San Potito Sannitico (Caserta, Italy). *Open Civ. Eng. J.* **2018**, *11*, 1106–1121. [CrossRef]
32. Benedetti, D.; Petrini, V. Sulla vulnerabilita sismica di edifici in muratura: Proposta su un metodo di valutazione. *L'Industria Delle Costr.* **1984**, *149*, 64–72. (In Italian)
33. Mosoarca, M.; Onescu, I.; Azap, B.; Onescu, E.; Chieffo, N.; Szitar-Sirbu, M. Seismic vulnerability assessment for the historical areas of the Timisoara city, Romania. *Eng. Fail. Anal.* **2019**, *101*, 86–112. [CrossRef]
34. Lagomarsino, S.; Giovinazzi, S. Macroseismic and mechanical models for the vulnerability and damage assessment of current buildings. *Bull. Earthq. Eng.* **2006**, *4*, 415–443. [CrossRef]
35. Apostol, I.; Mosoarca, M.; Chieffo, N.; Onescu, E. Seismic vulnerability scenarios for Timisoara, Romania. In *Structural Analysis of Historical Constructions*; Aguilar, R., Torrealva, D., Moreira, S., Pando, M., Ramos, L.F., Eds.; Springer: Berlin, Germany, 2019; pp. 1191–1200.
36. Lagomarsino, S. On the vulnerability assessment of monumental buildings. *Bull. Earthq. Eng.* **2006**, *4*, 445–463. [CrossRef]
37. Chieffo, N.; Clementi, F.; Formisano, A.; Lenci, S. Comparative fragility methods for seismic assessment of masonry buildings located in Muccia (Italy). *J. Build. Eng.* **2019**, *25*. [CrossRef]
38. Onescu, I.; Mosoarca, M.; Azap, B.; Onescu, E. Seismic Losses Scenario for Cultural Promenade in Timisoara Capital of Culture 2021, Romania. *IOP Conf. Ser. Mater. Sci. Eng.* **2019**, *471*, 102041. [CrossRef]
39. Toro, G.R.; Abrahamson, N.A.; Schneider, J.F. Model of Strong Ground Motions from Earthquakes in Central and Eastern North America: Best Estimates and Uncertainties. *Seism. Res. Lett.* **1997**, *68*, 41–57. [CrossRef]
40. Atkinson, G.M.; Kaka, S.L.I. Relationships between felt intensity and instrumental ground motion in the Central United States and California. *Bull. Seism. Soc. Am.* **2007**, *97*, 497–510. [CrossRef]
41. Crespellani, T.; Garzonio, C.A. Seismic risk assessment for the preservation of historical buildings in the city of Gubbio. In *Geotechnical engineering for the preservation of monuments and historic sites, Proceedings of the International Symposium on Geotechnical Engineering for the Preservation of Monuments and Historic Sites, Napoli, Italy, 3–4 October 1996*; Balkema: Rotterdam, The Netherlands, 1997.
42. Cauzzi, C.; Faccioli, E.; Vanini, M.; Bianchini, A. Updated predictive equations for broadband (0.01–10 s) horizontal response spectra and peak ground motions, based on a global dataset of digital acceleration records. *Bull. Earthq. Eng.* **2015**, *13*, 1587–1612. [CrossRef]
43. Esteva, D.; Harris, D.L. Comparison of pressure and staff wave gage records. *Coast. Eng. Proc.* **1970**, *1*, 7. [CrossRef]
44. Locati, M. DBMI15, the 2015 Version of the Italian Macroseismic Database, 2016. Available online: https://emidius.mi.ingv.it (accessed on 25 July 2019). (In Italian).
45. Grünthal, G. European Macroseismic Scale 1998. Available online: http://lib.riskreductionafrica.org/bitstream/handle/123456789/1193/1281.European%20Macroseismic%20Scale%201998.pdf?sequence=1 (accessed on 25 July 2019).
46. Onescu, I.; Onescu, E.; Mosoarca, M. Multi-criterial vulnerability assessment for Timisoara city, Romania. In Proceedings of the 4th International Conference on Structure and Architecture, Lisbon, Portugal, 24–26 July 2019.
47. Ferreira, T.M.; Vicente, R.; Varum, H. Seismic vulnerability assessment of masonry facade walls: Development, application and validation of a new scoring method. *Struct. Eng. Mech.* **2014**, *50*, 541–561. [CrossRef]
48. Chieffo, N.; Formisano, A. Geo-hazard-based approach for the estimation of seismic vulnerability and damage scenarios of the old city of senerchia (Avellino, Italy). *Geosciences* **2019**, *9*, 59. [CrossRef]

49. Ministerial Decree, DM 20/02/2018. "Updating of Technical Standards for Constructions". Available online: http://www.gazzettaufficiale.it/eli/gu/2018/02/20/42/so/8/sg/pdf (accessed on 25 July 2018). (In Italian).
50. Flemings, P.B.; Grotzinger, J.P.; Morris, J.E. Strata: A Stratigraphic Modeling Package, (n.d.). Available online: http://www.jsg.utexas.edu/flemings/intranet/software/strata/strata-download-the-code-manual-and-tutorial/ (accessed on 25 July 2019).